Contents lists available at ScienceDirect

Physics and Imaging in Radiation Oncology

Original Research Article

Individual lymph node position variation for rectal cancer patients treated with long course chemoradiotherapy

Dennis Tideman Arp [a,b,*], Ane L. Appelt [c,d], Rasmus Froberg Brøndum [e], Rasa Mikalone [f], Martin Skovmos Nielsen [a,b], Laurids Østergaard Poulsen [b,g]

[a] *Department of Medical Physics, Oncology, Aalborg University Hospital, Aalborg 9000, Denmark*
[b] *Department of Clinical Medicine, Aalborg University, Aalborg 9000, Denmark*
[c] *Leeds Institute of Medical Research at St James's, University of Leeds, Leeds LS2 9JT, UK*
[d] *Leeds Cancer Centre, St James's University Hospital, Leeds LS9 7TF, UK*
[e] *Center for Clinical Data Science, Aalborg University and Aalborg University Hospital, Aalborg 9000, Denmark*
[f] *Department of Radiology, Aalborg University Hospital, Aalborg 9000, Denmark*
[g] *Department of Oncology, Clinical Cancer Research Center, Aalborg University Hospital, Aalborg 9000, Denmark*

ARTICLE INFO

ABSTRACT

Background and purpose: Delivery of high precision radiotherapy lymph node boosts requires detailed information on the interfraction positional variation of individual lymph nodes. In this study we characterized interfraction positional shifts of suspected malignant lymph nodes for rectal cancer patients receiving long course radiotherapy. Furthermore, we investigated parameters which could affect the magnitude of the position variation.
Materials and Methods: Fourteen patients from a prospective clinical imaging study with a total of 61 suspected malignant lymph nodes in the mesorectum, presacral, and lateral regions, were included. The primary gross tumor volume (GTV$_p$) and all suspected malignant lymph nodes were delineated on six magnetic resonance imaging scans per patient. Positional variation was calculated as systematic and random errors, based on shifts of center-of-mass, and estimated relative to either bony structures or the GTV$_p$ using a hierarchical linear mixed model.
Results: Depending on location and direction, systematic and random variations (relative to bony structures) were within 0.6–2.8 mm and 0.6–2.9 mm, respectively. Systematic and random variations increased when evaluating position relative to GTV$_p$ (median increase of 0.6 mm and 0.5 mm, respectively). Correlations with scan time-point and relative bladder volume were found in some directions.
Conclusions: Using linear mixed modeling, we estimated systematic and random positional variation for suspected malignant lymph nodes in rectal cancer patients treated with long course radiotherapy. Statistically significant correlations of the magnitude of the lymph node shifts were found related to scan time-point and relative bladder volume.

1. Introduction

Radiotherapy (RT) is part of standard treatment for rectal cancer [1]; either as neo-adjuvant treatment (potentially combined with chemotherapy) to reduce risk of local recurrence after surgery [2,3], or as part of an organ-preservation treatment strategy. Standard RT regimens consists of either short course (25 Gy in 5 fractions) (SCRT) or long course radiotherapy (45–50.4 Gy in 25–28 fractions) (LCRT), to both tumor and elective lymph node regions. However, in some cases, the tumor [4–6] and possibly individual lymph nodes (LN) are escalated to higher doses (boost). LN dose escalation may be a supplement to surgery (e.g., LNs located in regions difficult to resect [7–9]) or part of a non-surgical management strategy.

Promising results and increasing experience with non-surgical management has increased the focus on treatment delivery precision in rectal cancer RT [10–12]. This includes appropriate use of planning target volume (PTV) margins, which requires solid understanding of target position variation during radiotherapy. Most studies of inter- and intra-fraction movement in rectal cancer have focused on primary tumor motion, however, with limited research done on individual LN motion.

While some studies have investigated this for other pelvic tumor sites [13–15], to our knowledge, no prior studies have investigated individual LN position variation for locally advanced rectal cancer patients receiving LCRT. This may be due to the poor visibility of LNs on standard on-treatment imaging, primarily cone-beam computed tomography (CBCT). Magnetic resonance imaging (MRI) is needed to ensure accurate delineation of all relevant pelvic LNs. A recent study by Kensen et al. [16] examined this specifically in a MRI-guided linear accelerator (MR-Linac) workflow for patients receiving SCRT with LNs located in the mesorectum. This still leaves out LNs in lateral and presacral areas, though, and is likely not representative for LCRT.

The aim of this study was to characterize and quantify interfraction shifts of suspected malignant LNs in LCRT treatment, in terms of systematic and random errors. Furthermore, to investigate the effect of LN anatomical location, scan time-point (pre- / during-treatment), bladder volume and match strategy on the magnitude of the position variation.

2. Materials and methods

2.1. Clinical study design

The study was based on a prospective clinical imaging study (AMPERE) of repeat MRI scans before and during radiotherapy for rectal cancer. Patients underwent six MRIs each (all on separate days); three before and three during the RT course (after one, two and four weeks). Inclusion criteria were patients referred to standard chemoradiotherapy for locally advanced rectal cancer. A full list of inclusion and exclusion criteria, and a flowchart showing the MRI schedule, is available in the supplementary material (Figure S.1.1 and Table S.1.2).

The MRI sequences used for tumor and LN visualization consisted of axial T2-weighted ($0.75 \times 0.75 \times 3$ mm^3), 3D T2-weighted ($1.5 \times 1.5 \times 1.5$ mm^3), 3D T1-weighted mDixon ($1.4 \times 1.4 \times 1.4$ mm^3) and diffusion weighted imaging (DWI)($2.5 \times 2.5 \times 4.0$ mm^3) acquired on a Philips Ingenia 3 T MRI scanner. The mDixon scans were part of a "MR-only" workflow package by Philips (MRCAT/MRPELVIS), which creates simulated computed tomography (CT) scans for RT dose calculation based on water-only, fat-only and in-phase mDixon sequences. For this study, the simulated CT was not used, just the fat- and water-only images. The scan package is approved for clinical use and the scans optimized with high resolution and geometrical accuracy [17]. Patients were instructed to empty their bladder before scanning in line with the department's standard clinical practice for radiotherapy planning and delivery. They were imaged in supine position, with identical fixation equipment for all scans, and hyoscinbutylbromid (antispasmodic to reduce bowel peristalsis) was administered prior to imaging if not contra-indicated.

The study protocol was approved by the Regional Scientific Ethics Committee for Northern Denmark (N-20170064), and the national Data Protection Agency. All patients provided written informed consent and the study was registered on ClincalTrials.gov (NCT03619668).

2.2. Patients and imaging

The study included 16 patients in the period 2018–2021 at Aalborg University Hospital, Denmark. Two patients were N0 and therefore excluded from this report. General patient characteristics for the 14 remaining patients are shown in Table 1. All patients completed the six MRI scans, resulting in 84 MRIs. The median time between each individual pre-treatment scans (MRI 1–3) were 4 days. The patients had between two and eight suspected malignant LNs identified. One patient had two LNs excluded, as they were impossible to identify on MRI scan 6. This resulted in a total of 61 LNs included in the analysis. The distribution and characteristics of the LNs and primary tumors are shown in Table 1 and visualized in Fig. 2. The mDixon sequence was updated during the inclusion period. Therefore, three patients had lower slice resolution (0.25 mm), which was retrospectively reconstructed to 0.11

Table 1

Patient, primary gross tumor volume (GTV$_p$) and lymph node characteristics. Lymph node volumes are calculated for all individual lymph combined.

Patient, GTV$_p$ and lymph node characteristics		
Number of patients		14
cT category	T2	1
	T3	8
	T4	5
cN category	N1	8
	N2	6
Age	Median (years)	63
	Interquartile range (years)	58–73
Sex	Female	8
	Male	6
Number of GTV$_p$		14
Location of GTV$_p$	Low (up to 5 cm)	11
	Mid (from 5 cm to 10 cm)	3
GTV$_p$ vol. at baseline	Median [cm^3]	28.2
	Interquartile range [cm^3]	16.8–53.2
Number of lymph nodes		61
Location of lymph nodes	Mesorectum	39
	Lateral lymph node region	11
	Pre-sacral	11
Lymph node vol. at baseline	Median [cm^3]	0.08
	Interquartile range [cm^3]	0.04–0.14

mm. All patients were treated with LCRT (50.4 Gy in 28 fractions) and concomitant chemotherapy with capecitabine. Treatment plans were delivered as 7 or 9-field intensity modulated radiotherapy (IMRT), applying daily image guidance radiotherapy (IGRT) with bony match and 6 degrees of freedom positioning (up to 3 degrees rotational compensation). No consolidation or induction chemotherapy was given.
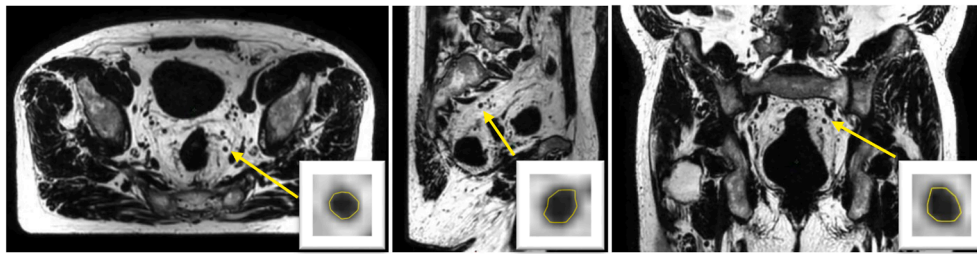
2.3. Lymph node delineations

Suspected malignant LNs were defined by expert gastrointestinal radiologists according to the diagnostic MRI and based on international consensus [18], and subsequently identified on the planning CT/MRIs. The LN volumes were delineated by an experienced radiographer on the mDixon MRIs. The fat-only images were used to delineate the LN volumes, since they show high contrast for precisely defining the edges of the LNs (see Fig. 1). Furthermore, the bladder was delineated on each scan using the water-only images.

2.4. Primary gross tumor volume (GTV) delineations

The primary tumor (GTV$_p$) was delineated using both the axial T2-weighted, 3D T2-weighted and DWI images to obtain the most accurate tumor representation. This was a multidisciplinary process involving a senior consultant oncologist, a senior consultant radiologist, and a medical physicist. All final delineations were reviewed and approved by the same consultant radiologist.

2.5. Image registration and position measurements

To characterize the relative position of the GTV$_p$ and LNs, the center-of-mass (COM) position was calculated for each structure on the baseline scan (MRI 1) using the departments clinical RT treatment planning system ARIA® (Varian Medical Systems, Palo Alto, CA). To facilitate this, MRI 2–6 were each rigidly co-registered on the bone structure regions to MRI 1; this was done by creating a mask around the bone structures, automatically segmented on the planning CT, and registering the MRIs based on grayscale values within the mask. The mask included the pelvic bone structures normally prioritized when using daily image

Fig. 1. Fat-only images from mDixon scan in axial (left), sagittal (middle) and coronal (right) view with a marked suspected malignant lymph node. The small, zoomed areas shows the delineation of the edges of the lymph node, which is clearly visible on the fat-only images in all three dimensions.
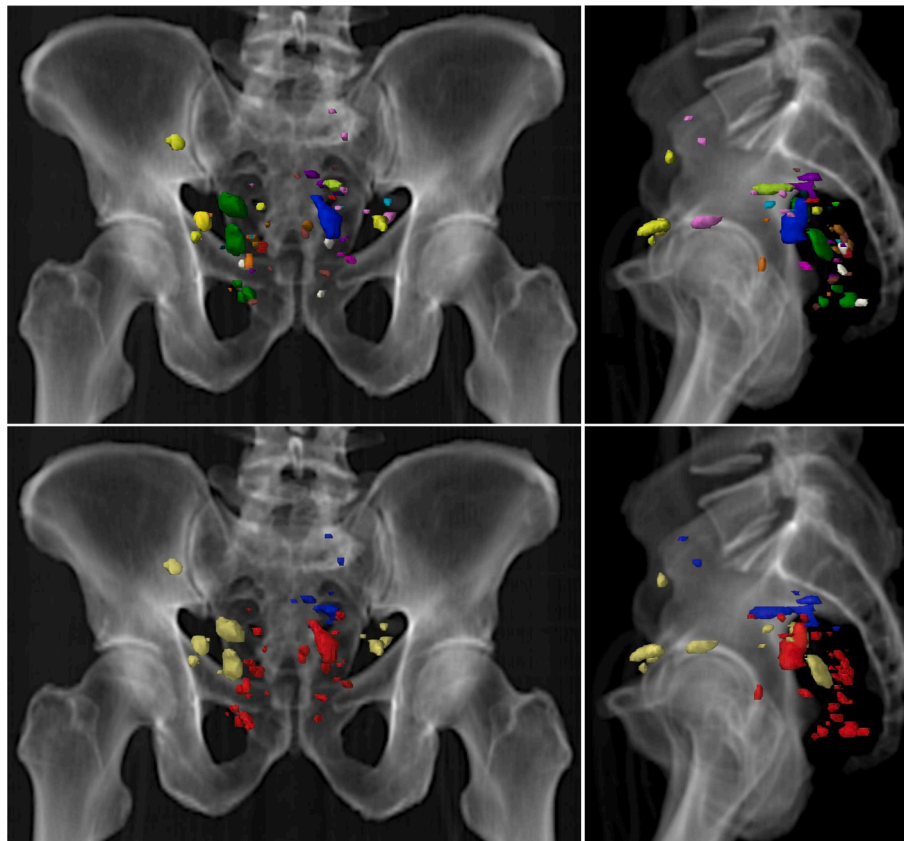
Fig. 2. Coronal (left) and sagittal(right) view of all 61 suspected malignant lymph nodes. Color coded for either patient (top) or by location (bottom, with meso-rectum [red], presacral [blue] or lateral pelvic region [yellow]). The lymph nodes were projected to one representative patient using a deformable registration with the bony structures on the planning CTs. The location and shape of the lymph nodes are approximative. (For interpretation of the references to color in this figure legend, the reader is referred to the web version of this article.)

guided radiotherapy (IGRT) with bone match. The registrations accounted for translational and rotational displacements (all within approximately 3 degrees), and all were visually evaluated. The rigid registrations were subsequently used to transfer each delineated GTV_p and LN to the baseline scan. LN locations were categorized as either mesorectal, presacral or lateral pelvic LNs (following the compartment definitions as described in the national Danish guidelines for RT of rectal cancer [19]). Measurements were labelled as either pre-treatment (MRI 2–3) or during-treatment (MRI 4–6). Relative bladder volumes were calculated as the difference for each MRI scan relative to the baseline (MRI 1).

2.6. Position variation and statistical analysis

Day-to-day position variation relative to bony structures was determined by calculating the relative shifts between the COM of the baseline

structures (GTV_p and each LN) and the corresponding transferred structures from MRI 2–6. This was done for each direction; left–right (LR), anterior-posterior (AP), and cranial-caudal direction (CC). Furthermore, the relative COM distance between each LN and the corresponding GTV_p (from the same scan number) was calculated, providing the shift relative to the GTV_p for individual LNs (i.e. the movement pattern of the LNs relative to that of the GTV_p).

COM shifts relative to bony structures (i.e. corresponding to setup using bony match on daily imaging) or relative to the GTV_p (i.e. corresponding to a soft tissue tumor match on daily imaging) were modelled using hierarchical linear mixed models with individual LNs nested within patients. We estimated systematic variation as the sum of variances allocated to the random effects of respectively the patient and LN effects, and random variation as the variation of residuals; for more details see supplementary material (S.1.3). The systematic and random standard deviation (SD) were estimated across all locations and

separately for each location (mesorectum, presacral, lateral).

The effects of location, baseline bladder volume, and the time-point of the scan (pre- / during-treatment) were tested by including each as a single fixed effect, while the relative bladder volume was included as a continuous covariate and tested stratified by location, to allow for differences in slope. Finally, a multivariable model including all covariates was fitted including an interaction between location and relative bladder volume. Due to the explorative nature of the study, p-values were not adjusted for multiple testing.

A full overview of the statistical data analysis, including the statistical code, is available for download at https://github.com/CLINDA-AAU/lymphnode_shifts.

3. Results

The magnitude of the LN shifts relative to bony structures were of the order 5 mm, except for a few outliers. A visual representation of the shifts is depicted in Fig. 3 for each patient grouped by the LN regions and in the supplementary material Figure S.1.4 for each individual LN.

Relative to the bony structures, LNs located in the mesorectum had a systematic variation in the range of 2.2–2.8 mm and random variation of 1.3–2.1 mm, depending on the direction. For the presacral LNs the systematic variations were 1.0–3.7 mm and random variations 1.4–2.2 mm. For LNs located in the lateral region, systematic variations in AP and CC direction were 0.6 mm and in the LR direction 2.3 mm. The random variations were 0.6–0.8 mm, depending on direction. For all LNs combined the variations were 2.0 mm (LR) / 2.4 mm (AP) / 2.9 mm (CC)

and 1.2 mm (LR) / 1.7 mm (AP) / 1.8 mm (CC) for systematic and random variations, respectively (see Table 2).

The magnitudes of the systematic and random LN positional variations increased for most estimates when considering the position relative to the GTV$_p$, with median increases of 0.6 mm and 0.5 mm, respectively. The group mean variations were between -1.5 mm to 0.5 mm relative to bony structures and -1.2 mm to 0.7 mm relative to the GTV$_p$.

Statistically significant differences of the magnitude of the LNs positional shifts relative to bony structures were observed in AP direction for pre-/during-treatment comparison ($p < 0.001$). This was also the case in the LR direction for lateral LNs ($p < 0.001$) and AP direction for the presacral LNs ($p = 0.016$) with relative bladder volume as covariate. Considering the relative bladder volume, a significant effect was found in the LR direction for lateral LNs, and in the AP direction for LNs located in the presacral space (Table 3). Similar results were seen for positional shifts relative to the GTV$_p$ (supplementary material Table S.1.5), and in the full multivariable model including all explored factors (supplementary material Table S.1.6).

4. Dicussion

In this study we examined interfraction shifts of suspected malignant LNs for patients with locally advanced rectal cancer treated with LCRT. This was done relative to bony structures and relative to the COM of the primary tumor, respectively. To our knowledge, only one other study has investigated individual LN positional variation for rectal cancer patients. Kensen et al. performed a study based on MR-Linac treatments
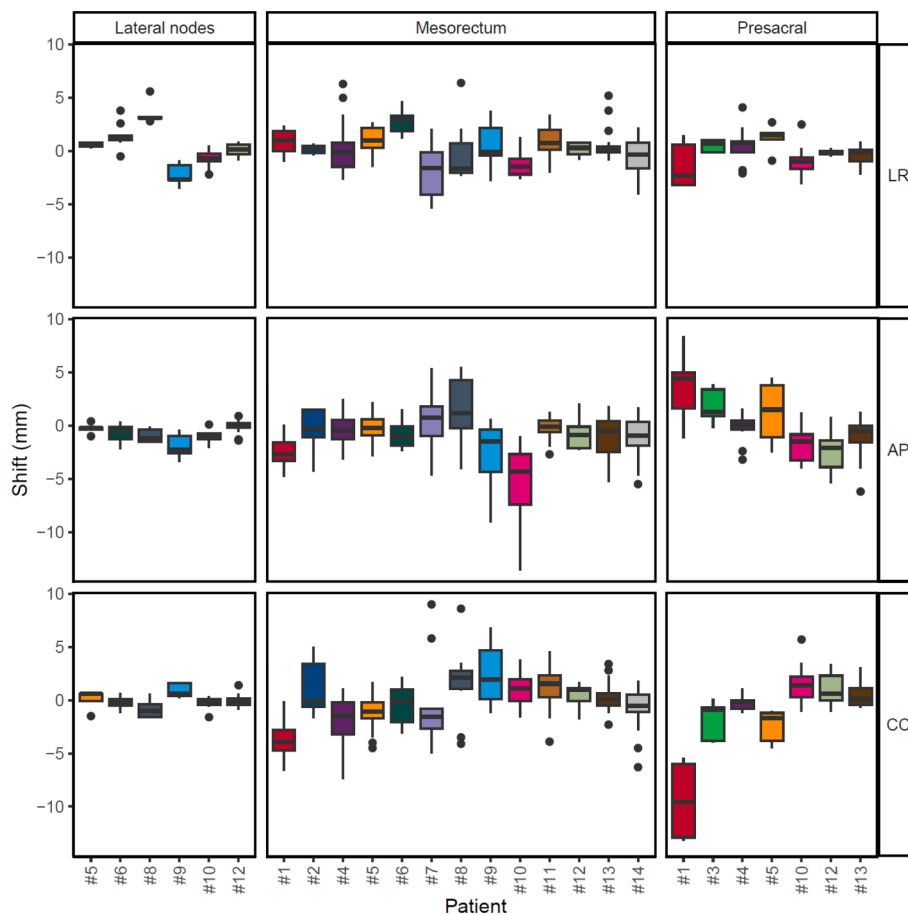
Fig. 3. Distribution of positional shifts, relative to bony structures, in each direction; left–right (LR), anterior-posterior (AP) and cranial-caudal (CC) for lymph nodes in lateral (left), mesorectum (middle) and presacral region. Each box represents a single patient (#1-#14) with data combining all lymph nodes in that region for that specific patient. The box plot depicts the median value (line), first and third quartiles (bottom and top of box), +/- 1.5*IQR (interquartile range, i.e. size of box) from the box (whiskers), and possible outliers (points).

Table 2
Systematic and random variation including group mean (GM) for positional shifts of lymph nodes relative to bony structures and primary tumor (GTVp), respectively.

Location (number)	Direction	Relative to bony structures			Relative to primary tumor		
		Systematic [mm]	Random [mm]	GM [mm]	Systematic [mm]	Random [mm]	GM [mm]
Mesorectum (n = 39)	LR	2.2	1.3	0.3	2.8	1.8	−0.2
	AP	2.8	1.8	−1.0	3.5	2.1	−0.5
	CC	2.2	2.1	0.0	2.6	2.4	0.5
Presacral (n = 11)	LR	1.0	1.4	−0.1	0.9	1.4	−0.4
	AP	1.9	2.2	0.1	2.7	2.6	−0.3
	CC	3.7	1.8	−1.5	3.2	2.2	−1.2
LLN (n = 11)	LR	2.3	0.8	0.5	1.9	1.3	−0.4
	AP	0.6	0.7	−0.8	1.8	1.8	0.0
	CC	0.6	0.6	−0.1	2.1	2.3	0.7
All combined (n = 61)	LR	2.0	1.2	0.2	2.5	1.7	−0.3
	AP	2.4	1.7	−0.7	3.2	2.2	−0.1
	CC	2.9	1.8	−0.4	3.1	2.4	0.0

Separated by anatomical location (mesorectum, presacral and lateral lymph nodes [LLN]) and direction (left–right [LR], anterior-posterior [AP] and cranial-caudal [CC]). For the GM, positive values correspond to shifts in the cranial, left and posterior direction.

Table 3
Effect of location, scan time, bladder volume on the magnitude of positional shifts relative to the bony structures as statistically estimated by linear mixed model.

		Left-right		Anterior-posterior		Craniel-caudal	
		Estimate [mm]	p-value	Estimate [mm]	p-value	Estimate [mm]	p-value
Effect of location	LLN (Intercept)	0 (reference)		0 (reference)		0 (reference)	
	Mesorectum	−0.01	0.99	−0.8	0.19	0.6	0.28
	Presacral	−0.33	0.60	0.2	0.75	0.4	0.57
Effect of Pre-/During	Pre-treat. (Intercept)	0 (reference)		0 (reference)		0 (reference)	
	During-treatment	0.1	0.39	−0.9	<0.01*	0.0	0.88
Effect of baseline bladder volume (per 100 mL)	Baseline bladder vol.	0.4	0.27	0.4	0.35	−0.0	0.98
Effect of relative bladder volume (per 100 mL)	LLN	1.0	<0.01*	−0.2	0.44	−0.0	0.81
	Mesorectum	0.0	0.94	−0.1	0.75	−0.2	0.50
	Presacral	0.2	0.65	−2.1	0.02*	1.2	0.11

Effects of location, Pre-/During-treatment scan and baseline bladder volume are modeled as contrasts relative to the intercept. LLN: Lateral lymph nodes. *Statistically significant p-values (<0.05).

using a daily adaptation workflow [16]. However, these patients were treated with SCRT and interfraction motion was only characterized assuming a soft tissue match on the primary tumor. While MR-Linac treatment offers great potential for soft tissue match and daily adaptation, the treatment modality is still associated with longer treatment times and MRI-related constraints, as well as limitations on access to treatment machines. Therefore, not all patients are eligible for daily adaptive MR-Linac treatment, and standard linac treatment will maintain relevance for most rectal cancer patients receiving radiotherapy.

The systematic and random variations (relative to primary tumor) found by Kensen et al. [16] were of the order 3–4 mm, except for the systematic variation in CC direction (6.3 mm). These were considerably larger than seen for mesorectal LNs in our study, especially in the CC direction. As Kensen and colleagues investigated SCRT, while the current study considered imaging during LCRT, this could indicate that treatment response during the LCRT course might reduce positional variation of the LN relative to the GTV_p. However, it might also be due to differences in the positional variation of the GTV_p, based on differences in the patient population and anatomical characteristics. Furthermore, differences in bladder filling protocol and the use of antispasmodic medication might also affect the variations. An empty bladder protocol might be more reproducible and result in smaller variations compared to a comfortably full bladder protocol [16,20,21]. Antispasmodic might influence the variations by reducing bowel peristalsis, however, to our knowledge, this does not substantially impact day-to-day variation. Other studies have explored the full LN regions (i.e. elective clinical target volumes) rather than individual LNs [21–26]. Nijkamp et al. [21] investigated interfraction shape variation of the mesorectum for rectal cancer patients treated with SCRT. They found heterogeneous shape variation with systematic variation up to 7.5 mm and random variation up to 4.8 mm, both in the anterior direction for the upper part of the mesorectum. Brierley et al. [26] investigated positional variation of the

whole mesorectal volume for rectal cancer patients treated with LCRT. They found a systematic variation of 1.1–1.8 mm and random variation of 1.5–2.0 mm for the LR direction and 1.9–2.2 mm (systematic) and 2.1–2.5 mm (random) for the AP direction. These are more comparable to our current study, but not necessarily fully correlated to the positional variation of individual LNs.

We estimated systematic and random variation of LNs relative to bony structures and relative to primary tumor using a hierarchical linear mixed model. Most studies investigating systematic and random variation for radiotherapy have used the definitions of systematic and random position variation as proposed by Van Herk et al. [27]. They thus define systematic variation(Σ) as the SD of the mean variation measured for each patient. The random variation(σ) is the corresponding root-mean-square of the SD of the measurements. However, this formulation is limited to single or independent sets of observations for each patient. Using a mixed modelling approach, which allows for multiple measurements from the same patient [28], we could include multiple LNs per patient and improve the strength of the observations. Considerable differences in LN positional variation relative to bony structures were observed across both locations and directions for systematic (0.6–3.7 mm) and random (0.6–2.2 mm) variances. This implies that different PTV margins could be applied when considering direction and location of the LNs. It is not straightforward to estimate to what extend the specific differences in variance contribute to the total optimal PTV margin, since this depends on the sum of all treatment related uncertainties (delineation uncertainties, intrafraction variation, etc.). However, considering positional variation only and using the simplified PTV calculation ($M_{PTV} = 2.5\Sigma + 0.7\sigma$) as proposed by Van Herk et al. [29], systematic and random variances of 0.6 mm (as seen in CC direction for lateral LNs) result in a PTV margin of 1.9 mm. In comparison, for presacral LNs, the PTV margin is 10.5 mm in the same direction, with systematic and random variances of 3.7 and 1.8 mm, respectively. LN

positional variation was also estimated relative to the GTV_p and showed an increase for both the systematic and random variances. This implies that larger nodal PTV margins might be necessary for a soft tissue match on the GTV_p compared to a bony match strategy. Furthermore, taking into consideration the results by Kensen et al. [16], it could indicate that adaptive treatment strategies might have added relevance when performing soft tissue match on primary tumor. It is important to note that the positional variation estimates found in this study do not take into account any additional delineation errors. In other words, they assume that the LNs are delineated geometrically accurate on the planning CT/ MRI and that rotational compensation is possible on the treatment unit. If not, this must be taken into account as additional uncertainties in the PTV margin calculation [30].

Furthermore, we investigated if location, scan time-point (pre- / during-treatment), baseline bladder volume and relative bladder volume effected the magnitude of the positional variation. Significant effects were found for the scan time-point (pre- /during- treatment) and relative bladder volume, for specific locations and directions. It is important to note that these statistical tests only estimate effects on the magnitude of the variation (i.e. differences in mean values) and therefore not necessarily directly affect the systematic and random variations. Furthermore, the relatively small number of observations (especially for the lateral and presacral LNs) makes the estimates sensitive to outliers; they must therefore be considered as indicative and need validation on larger patient cohorts.

This study was based on data from a prospective clinical imaging study with a balanced distribution of men and women. Furthermore, MRI scans offering high resolution and geometric accuracy were available for the definition of LNs and tumor. However, the clinical study included a limited number of patients and only six MRI scans were available per patient for analysis. Furthermore, most MRIs were before or early in the RT course (MRI 1–4) and therefore treatment effects might be underestimated. The number of patients and MRIs must therefore be considered as a limiting factor. Finally, the estimate of positional variation of the LNs relative to the primary tumor was based exclusively on a COM match. For more advanced tumors (as in this study), a COM match might not consider local changes and deformation.

In conclusion, we estimated positional variation for individual LNs for rectal cancer patient undergoing LCRT. This was done relative to bony structures and the primary tumor, respectively. Statistically significant effects on the magnitude of the shifts were found related to scan time-point and relative bladder volume.

CRediT authorship contribution statement

Dennis Tideman Arp: Conceptualization, Methodology, Software, Formal analysis, Investigation, Data curation, Writing – original draft, Writing – review & editing. **Ane L. Appelt:** Conceptualization, Methodology, Formal analysis, Writing – review & editing, Supervision. **Rasmus Froberg Brøndum:** Methodology, Software, Formal analysis, Writing – original draft, Writing – review & editing. **Rasa Mikalone:** Data curation, Writing – review & editing. **Martin Skovmos Nielsen:** Conceptualization, Methodology, Formal analysis, Writing – review & editing, Supervision. **Laurids Østergaard Poulsen:** Conceptualization, Methodology, Formal analysis, Writing – review & editing, Supervision.

Declaration of competing interest

The authors declare that they have no known competing financial interests or personal relationships that could have appeared to influence the work reported in this paper.

Acknowledgments

Appendix A. Supplementary data

Supplementary data to this article can be found online at https://doi. org/10.1016/j.phro.2024.100599.

References

[1] Glynne-Jones R, Wyrwicz L, Tiret E, Brown G, Rödel C, Cervantes A, et al. Rectal cancer: ESMO Clinical Practice Guidelines for diagnosis, treatment and follow-up. iv22–40 Ann Oncol 2017;28. https://doi.org/10.1093/annonc/mdx224.

[2] Kapiteijn E, Marijnen CA, Nagtegaal ID, Putter H, Steup WH, Wiggers T, et al. Preoperative radiotherapy combined with total mesorectal excision for resectable rectal cancer. N Engl J Med 2001;345:638–46. https://doi.org/10.1056/NEJMoa010580.

[3] Sebag-Montefiore D, Stephens RJ, Steele R, Monson J, Grieve R, Khanna S, et al. Preoperative radiotherapy versus selective postoperative chemoradiotherapy in patients with rectal cancer (MRC CR07 and NCIC-CTG C016): a multicentre, randomised trial. Lancet 2009;373:811–20. https://doi.org/10.1016/S0140-6736(09)60484-0.

[4] Gerard J-P, Barbet N, Schiappa R, Magné N, Martel I, Mineur L, et al. Neoadjuvant chemoradiotherapy with radiation dose escalation with contact x-ray brachytherapy boost or external beam radiotherapy boost for organ preservation in early cT2-cT3 rectal adenocarcinoma (OPERA): a phase 3, randomised controlled trial. Lancet Gastroenterol Hepatol 2023;8:356–67. https://doi.org/10.1016/S2468-1253(22)00392-2.

[5] Garant A, Vasilevsky C-A, Boutros M, Khosrow-Khavar F, Kavan P, Diec H, et al. MORPHEUS phase II-III study: A pre-planned interim safety analysis and preliminary results. Cancers 2022;14:3665. https://doi.org/10.3390/cancers14153665.

[6] Garcia-Aguilar J, Patil S, Gollub MJ, Kim JK, Yuval JB, Thompson HM, et al. Organ preservation in patients with rectal adenocarcinoma treated with total neoadjuvant therapy. J Clin Oncol 2022;40:2546–56. https://doi.org/10.1200/JCO.22.00032.

[7] Chen H, Nguyen KNB, Huang H, Feng C, Zhao X, Daly ME, et al. Effect and safety of radiation therapy boost to extramesorectal lymph nodes in rectal cancer. Pract Radiat Oncol 2020;10:e372–7. https://doi.org/10.1016/j.prro.2019.12.007.

[8] Hartvigson PE, Apisarnthanarax S, Schaub S, Cohen S, Bernier G, Koh W-J, et al. Radiation therapy dose escalation to clinically involved pelvic sidewall lymph nodes in locally advanced rectal cancer. Adv Radiat Oncol 2019;4:478–86. https://doi.org/10.1016/j.adro.2019.03.007.

[9] Meldolesi E, Chiloiro G, Giannini R, Menghi R, Persiani R, Corvari B, et al. The role of simultaneous integrated boost in locally advanced rectal cancer patients with positive lateral pelvic lymph nodes. Cancers (Basel) 2022;14. https://doi.org/10.3390/cancers14071643.

[10] Dossa F, Chesney TR, Acuna SA, Baxter NN. A watch-and-wait approach for locally advanced rectal cancer after a clinical complete response following neoadjuvant chemoradiation: a systematic review and meta-analysis. Lancet Gastroenterol Hepatol 2017;2:501–13. https://doi.org/10.1016/S2468-1253(17)30044-X.

[11] Verheij FS, Omer DM, Williams H, Lin ST, Qin L-X, Buckley JT, et al. Long-term results of organ preservation in patients with rectal adenocarcinoma treated with total neoadjuvant therapy: the randomized phase II OPRA trial. J Clin Oncol 2024; 42:500–6. https://doi.org/10.1200/JCO.23.01208.

[12] Appelt AL, Pløen J, Harling H, Jensen FS, Jensen LH, Jørgensen JCR, et al. High-dose chemoradiotherapy and watchful waiting for distal rectal cancer: a prospective observational study. Lancet Oncol 2015;16:919–27. https://doi.org/10.1016/S1470-2045(15)00120-5.

[13] Durrant L, Robinson M, Hawkins MA, Van den Heuvel F, Muirhead R. Quantifying target-specific motion in anal cancer patients treated with intensity modulated radiotherapy (IMRT). Radiother Oncol 2016;121:92–7. https://doi.org/10.1016/j.radonc.2016.08.011.

[14] Lawes R, Carter E, Hussein M, Murray J, McNair HA. Retrospective audit of inter-fraction motion for pelvic node radiotherapy in prostate cancer patients. Radiography 2021;27:266–71. https://doi.org/10.1016/j.radi.2020.08.002.

[15] Miriyala R, Rai B, Ballari NR, Oinam AS, Elangovan A, Singla V, et al. Prospective study to quantify expansion volumes around the involved pelvic lymph nodes to plan simultaneous integrated boost in patients with cervical cancer undergoing pelvic intensity modulated radiation therapy. Pract Radiat Oncol 2019;9:e394–9. https://doi.org/10.1016/j.prro.2019.02.006.

[16] Kensen CM, Betgen A, Wiersema L, Peters FP, Kayembe MT, Marijnen CAM, et al. Online adaptive MRI-guided radiotherapy for primary tumor and lymph node boosting in rectal cancer. Cancers 2023;15. https://doi.org/10.3390/cancers15041009.

[17] Philips. MRCAT Pelvis [datasheet]. https://www.documents.philips.com/asset s/20190730/51ac6ab3d4a640c1b05caa9a00cbe7b2.pdf?_ga=2.61367599.20 82097762.1715517764-1706559361.1715517764 (accessed May 12, 2024).

[18] Nougaret S, Reinhold C, Mikhael HW, Rouanet P, Bibeau F, Brown G. The use of MR imaging in treatment planning for patients with rectal carcinoma: have you checked the "DISTANCE"? Radiology 2013;268:330–44. https://doi.org/10.1148/radiol.13121361.

[19] Danish Colorectal Cancer Group. Vejledning til strålebehandling af rectum cancer. [Danish] 2020. https://dccg.dk/wp-content/uploads/2023/07/DCCG-Vejledning-ved-stralebehandling-af-cancer-recti.pdf (accessed May 12, 2024).

[20] Chang JS, Yoon HI, Cha HJ, Chung Y, Cho Y, Keum KC, et al. Bladder filling variations during concurrent chemotherapy and pelvic radiotherapy in rectal cancer patients: early experience of bladder volume assessment using ultrasound scanner. Radiat Oncol J 2013;31:41–7. https://doi.org/10.3857/roj.2013.31.1.41.

[21] Nijkamp J, de Jong R, Sonke J-J, Remeijer P, van Vliet C, Marijnen C. Target volume shape variation during hypo-fractionated preoperative irradiation of rectal cancer patients. Radiother Oncol 2009;92:202–9. https://doi.org/10.1016/j.radonc.2009.04.022.

[22] Kleijnen J-P-J-E, van Asselen B, Burbach JPM, Intven M, Philippens MEP, Reerink O, et al. Evolution of motion uncertainty in rectal cancer: implications for adaptive radiotherapy. Phys Med Biol 2016;61:1–11. https://doi.org/10.1088/0031-9155/61/1/1.

[23] Bondar L, Intven M, Burbach JPM, Budiarto E, Kleijnen J-P, Philippens M, et al. Statistical modeling of CTV motion and deformation for IMRT of early-stage rectal cancer. Int J Radiat Oncol Biol Phys 2014;90:664–72. https://doi.org/10.1016/j.ijrobp.2014.06.040.

[24] Yamashita H, Takenaka R, Sakumi A, Haga A, Otomo K, Nakagawa K. Analysis of motion of the rectum during preoperative intensity modulated radiation therapy for rectal cancer using cone-beam computed tomography. Radiat Oncol 2015;10:2. https://doi.org/10.1186/s13014-014-0311-6.

[25] Nijkamp J, Swellengrebel M, Hollmann B, de Jong R, Marijnen C, van Vliet-Vroegindeweij C, et al. Repeat CT assessed CTV variation and PTV margins for short- and long-course pre-operative RT of rectal cancer. Radiother Oncol 2012;102:399–405. https://doi.org/10.1016/j.radonc.2011.11.011.

[26] Brierley JD, Dawson LA, Sampson E, Bayley A, Scott S, Moseley JL, et al. Rectal motion in patients receiving preoperative radiotherapy for carcinoma of the rectum. Int J Radiat Oncol Biol Phys 2011;80:97–102. https://doi.org/10.1016/j.ijrobp.2010.01.042.

[27] van Herk M. Errors and margins in radiotherapy. Semin Radiat Oncol 2004;14:52–64. https://doi.org/10.1053/j.semradonc.2003.10.003.

[28] Matsuo Y, Nakamura M, Mizowaki T, Hiraoka M. Technical Note: Introduction of variance component analysis to setup error analysis in radiotherapy. Med Phys 2016;43:5195. https://doi.org/10.1118/1.4961397.

[29] van Herk M, Remeijer P, Rasch C, Lebesque JV. The probability of correct target dosage: dose-population histograms for deriving treatment margins in radiotherapy. Int J Radiat Oncol Biol Phys 2000;47:1121–35. https://doi.org/10.1016/s0360-3016(00)00518-6.

[30] Tudor GSJ, Bernstein D, Riley S, Rimmer Y, Thomas SJ, Van Herk M, et al. Geometric uncertainties in daily online IGRT. Br Inst Radiol 2020. https://doi.org/10.1259/geo-unc-igrt.